(a common phenomenon) and/or work by the brachiocephalicus muscle. We devised a five-segment computer simulation of the equine limb that had biceps represented by a spring ($k = 700$ kN m^{-1}) and recorded the joint angles at foot-off. The joint angular acceleration curves and segment trajectories generated by the simulation were very similar to those that we observed *in vivo* (see supplementary information).

The biceps released 243 J in 0.11 s in a gallop (2,200 W), which equates to a muscle with a peak power output of roughly 4,400 W (ref. 10). Equine muscle has a peak power output of about 90 W kg^{-1} ($V_{max} = 3.0$ lengths per second[5,6]; $F_{max} = 0.3$ MPa (refs 5, 9, 10); $a/P_0 = 2.5$ (ref. 5)). A horse would therefore require 50 kg of non-elastic muscle to achieve the same power output as a 0.4-kg biceps muscle. The peak power output of brachiocephalicus (identified as the main forelimb protractor[13]) would be only 220 W. The catapult mechanism is therefore essential for rapid protraction of the equine limb, and it is likely that similar mechanisms exist in other animals.

Alan M. Wilson*†, Johanna C. Watson*, Glen A. Lichtwark†

**Structure and Motion Laboratory, Department of Veterinary Basic Sciences, The Royal Veterinary College, Hatfield, Herts AL9 7TA, UK*
e-mail: awilson@rvc.ac.uk
†Institute of Human Performance, University College London, Stanmore, Middlesex HA7 4LP, UK

1. Weyand, P. G., Sternlight, D. B., Bellizzi, M. J. & Wright, S. *J. Appl. Physiol.* **89,** 1991–1999 (2000).
2. Pratt, G. W. & O'Connor, J. T. *Am. J. Vet. Res.* **39,** 249–253 (1978).
3. Hutchinson, J. R. & Garcia, M. *Nature* **415,** 1018–1021 (2002).
4. Schmidt-Nielsen, K. *Scaling: Why is Animal Size so Important?* (Cambridge Univ. Press, Cambridge, 1984).
5. Woledge, R. C., Curtin, N. A. & Homsher, E. *Monogr. Physiol. Soc.* **41** (Academic, London, 1985).
6. Rome, L. C., Sosnicki, A. A. & Goble D. O. *J. Physiol.* **431,** 173–185 (1990).
7. Alexander, R. McN. *Elastic Mechanisms in Animal Movement* (Cambridge Univ. Press, Cambridge, 1988).
8. Bennet Clark, H. C. *J. Exp. Biol.* **63,** 53–83 (1975).
9. Biewener, A. A. & Roberts, T. J. *Ex. Sport Sci. Rev.* **28,** 99–107 (2000).
10. Peplowski, M. M. & Marsh, R. L. *J. Exp. Biol.* **200,** 2861–2870 (1997).
11. Biewener, A. A. *Comp. Biochem. Physiol. B* **120,** 73–87 (1998).
12. Hermanson, J. W. & Hurley, K. J. *Acta Anat.* **137,** 146-156 (1990).
13. Dyce, K. M., Sack, W. O. & Wensing, C. J. G. (eds) *Textbook of Veterinary Anatomy* 2nd edn, 542–575 (Saunders, London, 1987).

Supplementary information accompanies this communication on *Nature*'s website.
Competing financial interests: declared none.

Outer planets

Origins of atmospheric zonal winds

The origin of the strong zonal (east–west) jets at cloud-top level in the atmospheres of Jupiter and Saturn[1] is something of a mystery[2,3]. Using an idealized two-dimensional, deep-turbulence model applied to a rapidly rotating planetary interior that is mixed by thermal convection, we are able to simulate the atmospheric multiple jets of these giant planets, and show that deep origins may explain one of their distinguishing features — the prograde (westerly) equatorial jets.

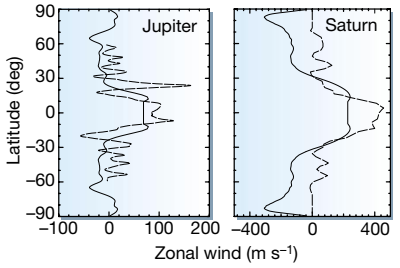

Figure 1 Simulated zonal winds (solid lines) and actual observations (dashed lines) for Jupiter and Saturn, after 300 and 100 planetary rotations, respectively, from an initial random state. Here, for numerical stability, spherical geometry is replaced by a cylindrical wall parallel to the axis of planetary rotation at 99% of the planetary radius, which intersects with the planetary surface at ±8.1° latitude. The plot assumes that homogeneous winds on this cylindrical wall are directly observed at the cloud tops of the lower latitudes. Full modelling details are available from the authors.

This feature cannot be reproduced in conventional shallow-atmosphere models. A set of idealized simulations of single fluid-layer flows on a rotating sphere, starting from a random initial condition[4], explains both the magnitude and the number of jets well, but has an important defect in that it produces retrograde (easterly) jets at the equator. The reason for this defect is that turbulent horizontal mixing of the planetary rotational vorticity, which has opposite signs in the two hemispheres, gives rise to a slower (retrograde) atmospheric rotation than the planetary value over the equator. The sign of the parameter β, defined as the rate of change of the Coriolis parameter with latitude, dictates the sign of the jets (see equation (2.4) in ref. 5) by the conservation of potential vorticity[6], which measures the total strength of the atmospheric vorticity tube, in the course of this mixing process[7].

The atmospheres of Jupiter and Saturn are much deeper than Earth's atmosphere, however, making possible completely different dynamics[8–10] in which the flows are deep, extending from one hemisphere to another. These flows are homogeneous in the direction of the axis of planetary rotation when the planetary interior is well mixed by thermal convection[8]. A single fluid layer, confined within the planetary sphere, therefore describes these deep flows[10].

Analogous dynamics that conserve a potential vorticity govern this system, which is defined in terms of the deep fluid tubes parallel to the axis of planetary rotation. The resulting β, which now measures the rate of change in the length of fluid tubes with latitude, takes the opposite sign[2,9]. Consequently, the equatorial jet also has an opposite sign, as has been observed. Lateral transport of stronger potential vorticity, owing to longer fluid tubes, from higher latitudes to the equator, gives rise to faster (prograde) rotation.

To demonstrate this, we run the model, assuming constant density and no convective buoyancy forcing, for a long period, starting from a random state with wind variance of 100 m s^{-1} and 200 m s^{-1} for Jupiter and Saturn, respectively. These magnitudes are comparable to those observed[1,4]. In both cases, we obtain the prograde equatorial jets of the correct width and magnitude, and also with an indication of multiple jets (Fig. 1).

Another attractive feature of our 'deep' model is that the magnitude of β values is greater, which relaxes the wind-shear stability criterion[9] and opens the way for obtaining steeper high-latitude jets, in accordance with observations. This is another feature that conventional shallow models can reproduce only with difficulty. Inclusion of a convective buoyancy force[8] would give rise to steeper jets in our deep model.

Jun-Ichi Yano*, Olivier Talagrand†, Pierre Drossart‡

**Laboratoire de Météorologie Dynamique, École Polytechnique, F-91128 Palaiseau, France*
e-mail: yano@cnrm.meteo.fr
†LMD, Ecole Normale Supèrieure, F-75231 Paris, France
‡LESIA (CNRS-FRE2461), Observatoire de Paris, F-92125 Meudon, France

1. Ingersoll, A. P. *Science* **248,** 308–315 (1990).
2. Yano, J.-I. *Chaos* **4,** 287–297 (1994).
3. Ingersoll, A. P., Gierasch, P. J., Banfield, D., Vasavada, A. R. & Galileo Imaging Team *Nature* **403,** 630–632 (2000).
4. Cho, J. Y.-K. & Polvani, L. M. *Science* **273,** 335–337 (1996).
5. Yano, J.-I. & Flierl, G. R. *Dyn. Atmos. Ocean* **16,** 439–472 (1992).
6. Pedlosky, J. *Geophysical Fluid Dynamics* 2nd edn (Springer, New York, 1987).
7. Rhines, P. B. & Young, W. R. *J. Fluid Mech.* **122,** 347–367 (1982).
8. Busse, F. H. *Icarus* **29,** 255–260 (1976).
9. Ingersoll, A. P. & Pollard, D. *Icarus* **52,** 62–80 (1982).
10. Yano, J.-I. & Flierl, G. R. *Ann. Geophysicae* **12,** 1–18 (1994).

Competing financial interests: declared none.